A&A 430, 263–278 (2005)
DOI: 10.1051/0004-6361:20034547

Astronomy & Astrophysics

Radial velocity variations in pulsating Ap stars

IV. First results on HR 1217⋆

D. E. Mkrtichian[1,2] and A. P. Hatzes[3]

[1] Astrophysical Research Center for the Structure and Evolution of the Cosmos, Sejong University, Seoul 143-747, Korea
e-mail: david@arcsec.sejong.ac.kr
[2] Astronomical Observatory, Odessa National University, Shevchenko Park, Odessa 65014, Ukraine
[3] Thüringer Landessternwarte Tautenburg, Sternwarte 5, 07778 Tautenburg, Germany
e-mail: artie@tls-tautenburg.de

Received 21 October 2003 / Accepted 28 June 2004

Abstract. In this paper we present the first results from a high-precision radial velocity (RV) study of the rapidly oscillating Ap (roAp) star HR 1217. Data spanning a complete rotation period were acquired on 9 nights in late 1997 and early 1998 using the Harlan J. Smith 2.7 m telescope at McDonald Observatory. The RVs were measured using the wavelength range of each spectral order (≈100 Å) of the "2dcoude" echelle spectrograph. Most of the pulsational modes can be seen in all spectral regions but the amplitude varies by factors of ten or more between the different wavelength intervals. A detailed analysis of the spectral order centered on 5825 Å, which had the largest amplitudes, showed the presence of all published photometric frequencies f_1–f_7. The multi-mode oscillations were also found in the RV variations of the high amplitude Nd III 5294 Å feature. Our RV data reveal two new excited modes at frequencies $f_0 = 223.37$ c d^{-1} (2585.3 μHz) and $f_{-1} = 220.58$ c d^{-1} (2553.0 μHz) that follow the odd and even alternative mode spacing with $\Delta\nu_0/2 \simeq 34$ μHz. An analysis of individual nights shows strong amplitude and phase modulation of all excited modes, including the two newly discovered ones. The amplitudes of the $f_2 = 229.21$ c d^{-1} (2652.9 μHz) and $f_4 = 235.08$ c d^{-1} (2720.85 μHz) modes are modulated with the published magnetic field variations and reach their maximum and minimum at magnetic extrema. However, the phase variability is in disagreement with that expected from the standard oblique pulsator model. The phase jumps for the f_2 mode occur exactly at magnetic maximum and close to the phase of magnetic minimum, while the f_3 and f_4 modes have a continuous change. The peculiar phase variability is attributed to strong vertical phase changes in the line-forming layers of atmosphere. An echelle-diagram for all known excited modes in HR 1217 is constructed. We interpret the $f_7 = 242.41$ c d^{-1} (2805.7 μHz) mode with the "peculiar" spacing as due to a mode of degree $l = 4$ that is the only observed member of another system of equally-spaced frequencies. We predict the existence of modes belonging to this system that should be equally spaced at 68 μHz with f_7.

Key words. techniques: radial velocities – techniques: spectroscopic – stars: chemically peculiar – stars: oscillations – stars: individual: HR 1217

1. Introduction

Magnetic chemically-peculiar (Ap) stars are a class of late B through late A-type stars that show strong magnetic fields with strengths of up to several kiloGauss. These stars also exhibit strong surface chemical peculiarities with many elements having a patchy distribution across the stellar surface. The photometric, spectroscopic, and magnetic variability in Ap stars are due to rotational modulation. In the case of the magnetic field variations these are due to the inclination of the magnetic axis with respect to the rotation axis. The magnetic fields are also believed to be responsible for the surface chemical inhomogeneities.

The rapid oscillations, both mono- and multi-periodic, with periods of 5 to 16 min and typical photometric amplitudes less then a few mmag were discovered in cool Ap stars by Kurtz (1978) and interpreted (Kurtz 1982) as due to high-overtone zonal dipole ($l = 1$, $m = 0$) p-modes with their axis of symmetry coinciding with the magnetic axis. The obliquity of the pulsation axis produces rotational modulation in both the phase and amplitude of the pulsations as predicted by the so-called "oblique pulsator model" or OPM (Kurtz & Shibahashi 1986; Takata & Shibahashi 1995; Dziembowski & Goode 1996). We shall refer to this standard model and its revisions (Bigot & Dziembowski 2002) as the "two-dimensional oblique pulsator models" (2D-OPM) because these are based on the assumption that the amplitudes and phases of stellar nonradial pulsation brightness and velocity fields depend *only* on the stellar latitude and longitude.

The relatively rich p-mode spectra of some roAp stars makes these objects attractive for asteroseismic studies.

⋆ Based on observations made at McDonald Observatory.

Fig. 1. The pulsational radial velocity curves of HR 1217. The solid lines are the nightly synthetic multifrequency fits.

The spacing of modes in the multiperiodic roAp pulsators are well represented by the asymptotic relationship for the frequency spacing of low l-degree high-overtone ($n > 15$) acoustic modes (Tassoul 1990).

$$\nu_{n,l} = \Delta\nu_0 \left(n + \frac{l}{2} + \epsilon \right) + \delta\nu \quad (1)$$

where ϵ is a small constant depending on the star's structure and $\delta\nu$ is the so called "small spacing" – a small term that is sensitive to the central structure of the star. The term $\Delta\nu_0$ is the frequency spacing between the consecutive overtones and is the inverse of the sound crossing time across the stellar diameter with a variable sound speed $c(r)$

$$\Delta\nu_0 = \frac{1}{2\int_0^R \mathrm{d}r/c(r)} \quad (2)$$

and is often called the "large separation". For main sequence stars with mass between 1.0 and 2.0 $M_\odot$ $\Delta\nu_0$ can be calibrated as

$$\Delta\nu_0 = 0.205 \left(\frac{GM}{R^3} \right)^{1/2} \quad (3)$$

with an accuracy better than 10% (Gabriel et al. 1985). It is a good measure of the displacement of an roAp star from the main sequence in the color-magnitude diagram. Matthews et al. (1999) found general agreement between the asteroseismic and geometric (*Hipparcos*) parallaxes, but the *Hipparcos* distances were systematically larger than predicted by asteroseismology.

The sharp-lined roAp star HR 1217 (HD 24712, DO Eri) is a typical member of the cool group of Ap stars. It shows rotationally modulated magnetic field variability with a strength ranging from +0.4 kG to 1.5 kG (Preston 1972) and has a rotation period of 12.4572 days (Kurtz & Marang 1987). Bangulo et al. (1995), using combined linear and circular polarization data, found a polar magnetic field of $B_P = 3.9$ kG, an inclination angle to the line-of-sight of $i = 137°$, and an obliquity angle (the angle between the rotation and magnetic axes) of $\beta = 150°$. The error in the angle determination is 2°–3°. Leroy et al. (1996), based on linear polarization measurements, estimated $i = 140 \pm 5°$ and $\beta = 147 \pm 5°$, consistent with the Bangulo et al. (1995) determinations.

HR 1217 shows strong variations in the spectral lines of Eu with a maximum coinciding with magnetic maximum and Mg lines that vary antiphase with Eu (Preston 1972). The detailed abundance analysis of HR 1217 (Ryabchikova et al. 1997) shows an underabundance of most the iron-peak elements and an overabundance of rare earth elements and cobalt. The rare earth elements show large equivalent width variations over the rotation period and abundance variations of about 0.5 dex. Magnesium is at solar abundance, but is deficient by about 1.0 dex at magnetic minimum. These confirm the inhomogeneous distribution of some elements across the surface of this star.

The rapid and multimode pulsations in HR 1217 were discovered by Kurtz (1982) and have been well studied (Kurtz & Seeman 1983; Kurtz et al. 1989). The frequency spectrum was found to have 6 principal frequencies that show rotationally modulated amplitude variations. The first five are spaced in frequency alternately by 33.27 μHz and 34.75 μHz.

Shibahashi (1984) was the first to explain that the observed frequencies are equally spaced due to alternative odd and even l-modes with a principal spacing $\Delta\nu_0 = 68\,\mu$Hz. However, the sixth mode at frequency 2806.2 μHz was found at a spacing of $\Delta\nu = 49.99\,\mu$Hz from the $f_5 = 2755.4\,\mu$Hz mode. This mode was termed "enigmatic" by Kurtz et al. (1989).

Mkrtichian & Hatzes (2000) gave a possible explanation of the peculiar spacing of the 2806.2 μHz mode with respect to f_5. This is due to a higher degree $l > 3$ mode that is naturally shifted in spacing relative to the sequence of $l = 0$, 2 (even) and $l = 1$, 3 (odd) sequence that form the equal spacing of the observed f_1–f_5 modes.

Another possible explanation of the peculiar spacing of 2806.2 μHz was suggested by Cunha (2001) who proposed that the mode following the fifth mode was actually missing from observations due to its coupling with Alfv́enic waves at the surface of the star. The next mode that is observed has its frequency diminished by the effect of the magnetic field.

Recently, using a global multisite campaign on HR 1217 with the *Whole Earth Telescope*, Kurtz et al. (2002) found the "missing" mode at a frequency $f_6 = 2791.48$ μHz. This was separated from f_5 by 36.13 μHz and thus followed the f_1–f_5 alternative odd and even degree spacing. The spacing of the 2806.2 μHz mode remains unexplained.

The first spectroscopic detection of pulsations in HR 1217 were reported by Matthews et al. (1988) who found radial velocity (RV) variations with a peak-to-peak amplitude of 400 m s^{-1} on one night, but were unable to detect any significant variations on the previous night to a level of 130 m s^{-1}. The first spectroscopic RV confirmation of the multimode pattern of oscillations in HR 1217 were found by Hatzes et al. (1999, 2002). In the preliminary analysis of their data they detected five of the six photometric modes known at that time and these showed strong amplitude variations from night to night. Balona & Zima (2002), based on high-resolution spectroscopy of HR 1217, found radial velocity variations with power in the 2.6–2.8 mHz range. However, the strong 1 c d^{-1} aliasing in the power spectrum and the low signal-to-noise ratio of the data did not permit the accurate discrimination of multi-mode oscillation frequencies.

Mkrtichian (1992, 1994) introduced for the study of the two-dimensional (l, m) structure of nonradial pulsations in roAp stars the concept of a "periodic spatial filter" (hereafter 2D-PSF). The distribution of chemical elements on the surface of Ap stars is known to be patchy. Pulsational RV variations originating from an element concentrated in a localized region of the star will experience less cancellation effects allowing higher degree modes to be detected. Thus spectroscopic studies are more sensitive and have the potential of finding higher degree modes than are possible using photometric studies which measure a more "integrated" quantity.

In this paper we present preliminary results of our RV study of the pulsations in HR 1217. The RV analysis is primarily performed on a wavelength interval spanning each spectral order of the echelle spectrograph employed for this study (≈100 Å).

Table 1. Log of the 1997/1998 year spectroscopic observations. The rotation phases are given according to ephemeris of Kurtz et al. (1989). N is the number of RV points obtained per night.

Date	HJD 2450000+		Phase	N
(UT)	Start	End		
16 Dec. 97	798.6183	798.8618	0.4817	228
17 Dec. 97	799.6112	799.8737	0.5621	277
18 Dec. 97	800.6047	800.8578	0.6415	269
19 Dec. 97	801.6182	801.8630	0.7225	263
20 Dec. 97	802.6104	802.7793	0.7991	169
22 Dec. 97	804.6091	804.8561	0.9627	258
30 Jan. 98	843.5753	843.7571	0.0881	156
1 Feb. 98	845.5556	845.7688	0.2483	236
2 Feb. 98	846.5714	846.7700	0.3293	219

These are termed "broad-band" RV measurements as they represent an average RV from many lines. Previous work (Kanaan & Hatzes 1998; Mkrtichian et al. 2003; Hatzes & Mkrtichian 2004) has shown that a more complete understanding of the pulsational RV variations in roAp stars can only come after an examination of the RV variations of individual lines. This type of study is a time consuming process and will be the subject of a subsequent paper. In this work we concentrate on the broad-band RV measurements and present a detailed analysis of only one spectral order and one spectral feature of Nd III. We show that even with these broad-band and single-line measurements we are able to find the presence of additional excited modes.

2. Observations and reduction

Observations of HR 1217 were made using the "2dcoude" spectrograph (Tull et al. 1995) of the 2.7-m telescope at McDonald Observatory on the nights 16–19, 20, 22 December 1997, 30 January 1998, and 1, 2 February 1998. These nights cover a complete rotation period of the star with good phase sampling. One focus of the instrument provides a resolving power $R(=\lambda/\Delta\lambda) = 60\,000$ with a nominal wavelength coverage of 4000–10 000 Å in one exposure when used with a Tektronix 2048×2048 CCD detector. To improve the duty cycle of the observations the CCD was binned by a factor of two perpendicular to the dispersion direction and framed so that only pixels covering the wavelength range 4700–7000 Å were recorded. This procedure resulted in a total dead time (CCD readout and data storage) of 15 s. Exposure times were typically 35 s resulting in a full duty cycle of 50 s. The journal of observations is given in Table 1 which lists the JD start and end of the observing sequence and the number of spectra that were obtained on each night.

Precise stellar radial velocity measurements were made using an iodine absorption cell placed just before the entrance slit of the spectrograph during each observation. A description of the use of this method can be found in Hatzes & Kürster (1994). This analysis did not take into account possible changes in the shape of the instrumental profile which is required if one wants to achieve the very highest RV precision (Valenti et al. 1995; Butler et al. 1996). This was not done because this is computationally intensive given the large number of observations. Furthermore, the expected RV variations are large (50–300 m s^{-1}) and should not be influenced by subtle changes of the instrumental profile.

Molecular iodine has useful lines in the wavelength range of 5000–6300 Å (14 spectral orders) which dictated the subframing of the CCD detector. The RV analysis with the iodine cell requires a high signal-to-noise template spectrum of the star taken without iodine absorption lines. For this we took a much longer exposure of HR 1217 without the cell. Figure 1 shows sample radial velocity curves from a single spectral order at the observed rotation phases.

3. Time-series analysis

A time series analysis using discrete Fourier transforms (DFT) was performed on the RV measurements. Throughout the paper we follow the nomenclature of frequencies f_1–f_7 given in a recent paper of Kurtz et al. (2002) that is different from earlier nomenclature f_1–f_6 (Kurtz et al. 1989). The old ("enigmatic") f_6 is denoted as f_7, while the current f_6 is the new photometric mode found by Kurtz et al. (2002). With this convention the numerical subscript is consistent with an increasing value of frequency. Following this nomenclature we denote the new spectroscopically detected frequencies as f_0 and f_{-1} in order to compare with previous works. Note that the negative subscript should not be confused with the negative superscript normally used to denote rotational sidelobes. Rather, it gives a relative frequency location with respect to other published modes.

Our RV analysis software uses days as the time unit, so the results of our DFT analysis produces frequencies as cycles per day. We relate these frequencies to the more conventional μHz unit when necessary.

3.1. Analysis of all the spectral orders

Figures 2 and 3 show the discrete Fourier transform of the RV variations for each of the 14 spectral orders (left to right) as a function of rotation phase (top to bottom). The number above each column of DFTs represents the central wavelength of the spectral order. Each order spans approximately ±50 Å from the central wavelength. Rotation phases were reckoned according to

$$\mathrm{JD} = 2\,446\,744.15 + 12.4572E$$

(Kurtz et al. 1989) where phase 0.0 corresponds to the maximum of the photometric variations. This is also near the phase of magnetic maximum (Kurtz et al. 1989). We will not discuss in the present paper the accuracy of this ephemeris or try to improve it.

There are strong amplitude variations both as a function of wavelength and rotation phase. The highest RV amplitudes can be found in the spectral region centered on 5825 Å where the amplitude can be as high as 200 m s^{-1}. This is most likely due to the contribution of high-amplitude of rare earth element (REE) lines that lie inside the spectral order (for instance Nd III 5845.02 Å). Studies have shown that these can have the highest RV amplitudes (Savanov et al. 1999; Kochukhov & Ryabchikova 2001a,b; Balona & Zima 2002). The same is true

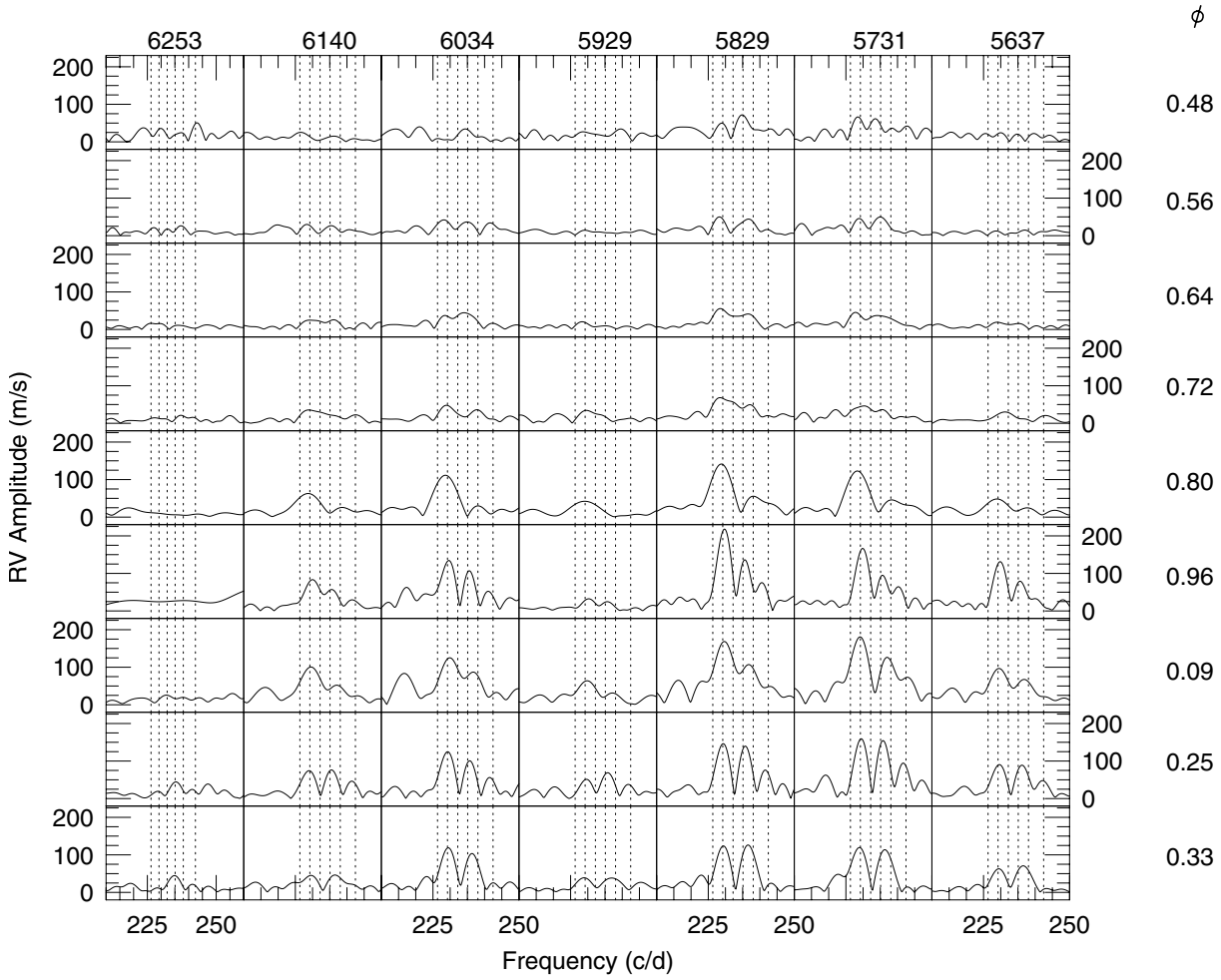

Fig. 2. The discrete Fourier transform (central wavelength shown at the top) as a function of rotation phase (*top to bottom*, rotation phase values shown at the far right) for the first 7 spectral orders (wavelength interval 5590–6300 Å). Each spectral order spans approximately 100 Å. The dashed lines show the location of the published photometric frequencies from Kurtz et al. (1989).

for other spectral orders centered on 5056 Å and 5132 Å showing high amplitude RV variations (up to 100 m s^{-1}). The lowest amplitude spectral regions are centered on 6253 Å and 5929 Å where the amplitude often does not exceed about 40 m s^{-1}.

There are also very strong amplitude variations associated with rotational modulation. The highest amplitudes occur in the phase interval $0.8 < \phi_{\rm rot} < 1.3$ where the pulsational modes can be seen in all spectral orders, with the possible exception of the one centered on 6253 Å. The center of this phase interval coincides with magnetic maximum. The pulsational RV amplitude of all modes are low, or non-detectable between the phase interval $0.3 < \phi_{\rm rot} < 0.8$ which is coincident with the minimum of the magnetic field variations.

The dominant mode in all the power spectra of the various spectral orders appears to be $f_2 = 229.22$ c d^{-1} (2653 μHz). To show the rotational modulation of the pulsational phase and amplitude a least squares fit using this single frequency was made to all the RV data. Throughout this paper the pulsational phase, ϕ in fraction of a pulsation cycle, is calculated according to the sin-wave fit $RV(t) = RV_0 + K \cdot \sin\ 2\pi(f \cdot (t - T_0) + \phi)$ with an arbitrary starting time, T_0 = HJD 2 450 000.

We chose not to fit all the modes for every spectral order as this is time consuming and of limited use for atmospheric diagnostics since more information can be gleaned from a RV analysis using single spectral lines. (Below we perform a detailed analysis of a single spectral order.) However, it would be instructive to see the amplitude and phase modulation for a single high-amplitude mode for all spectral regions since this provides the best comparison to very broad-band (compared to this study) photometric variations.

Figures 4 and 5 show the variations of the phase and amplitude, respectively, of the f_2 mode as a function of rotation phase. The reddest order (centered on 6253 Å) is not shown because the pulsational amplitude and phase could not be determined with sufficient accuracy due to a poor measurement precision caused by two effects. First, the iodine absorption lines are quite weak in this spectral order and they lose their efficacy as a wavelength reference. Second, this region of the spectrum was plagued by many telluric absorption features which can add systematic errors to the RV measurements.

The amplitudes and phases of the various modes and their rotational sidelobes when analysing the complete data set does not give us direct information about the shape of the amplitude

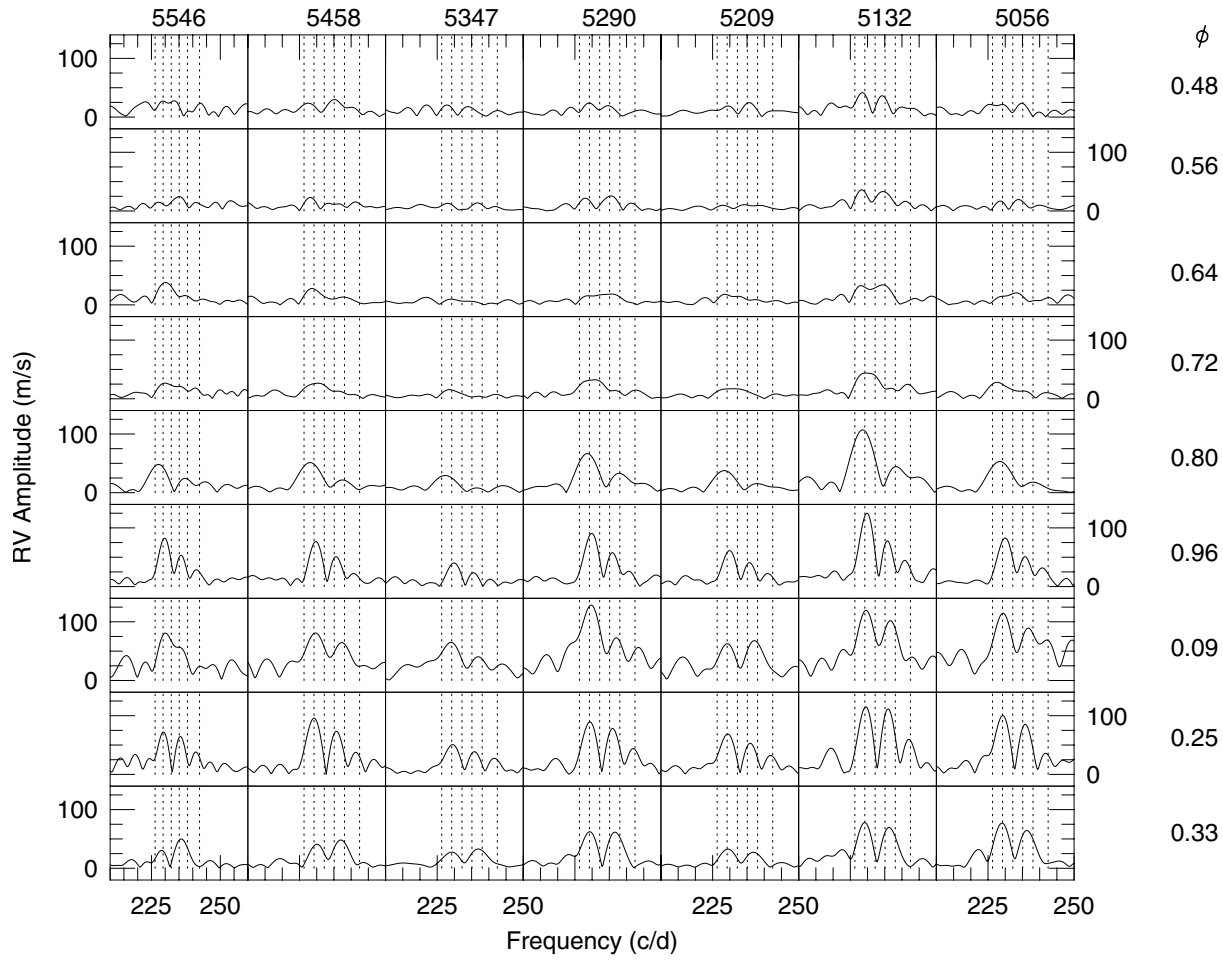

Fig. 3. The same as in Fig. 2, but for the wavelength interval 5013–5590 Å (7 spectral orders).

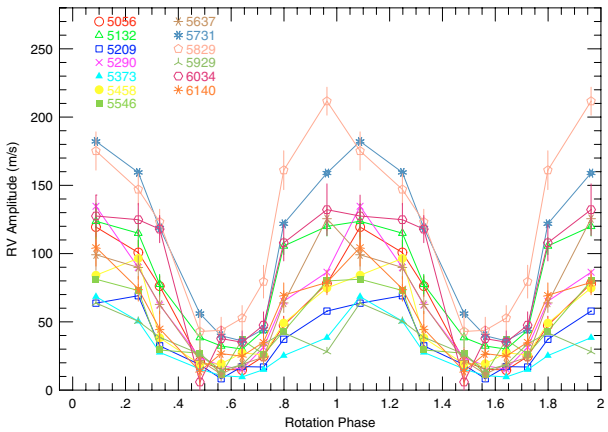

Fig. 4. The rotational modulation of the amplitude of the f_2 = 229.21 c d^{-1} (2653 μHz) mode for each of the spectral regions (orders).

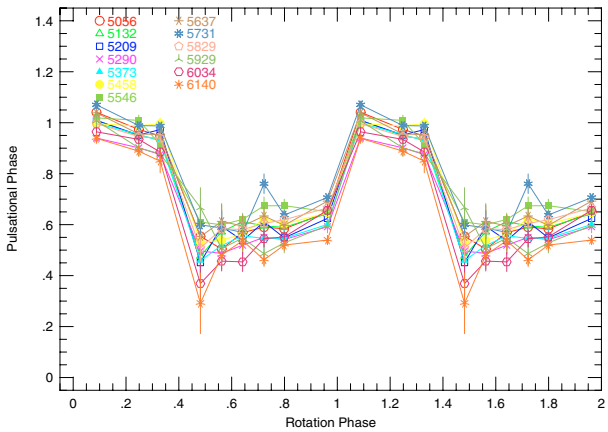

Fig. 5. The rotational modulation of the phase of the f_2 = 229.21 c d^{-1} (2653 μHz) mode for each of the spectral regions (orders). Symbols are the same as for Fig. 4. The pulsation phase is given in fractions of a pulsation cycle.

modulation and the rotational phases of pulsation phase jumps of the individual modes. The "averaged" amplitudes of modes over a complete rotation cycle will be significantly lower than the maximum from an individual night. These averaged amplitudes might also miss some as yet undetected mode whose signal may be present at one rotation phase, but not another. For these reasons we divided our analysis into three steps.

First, the entire data set of one spectral order was studied in detail. We chose to perform this broad-band RV analysis on the high-amplitude order centered on wavelength 5825 Å.

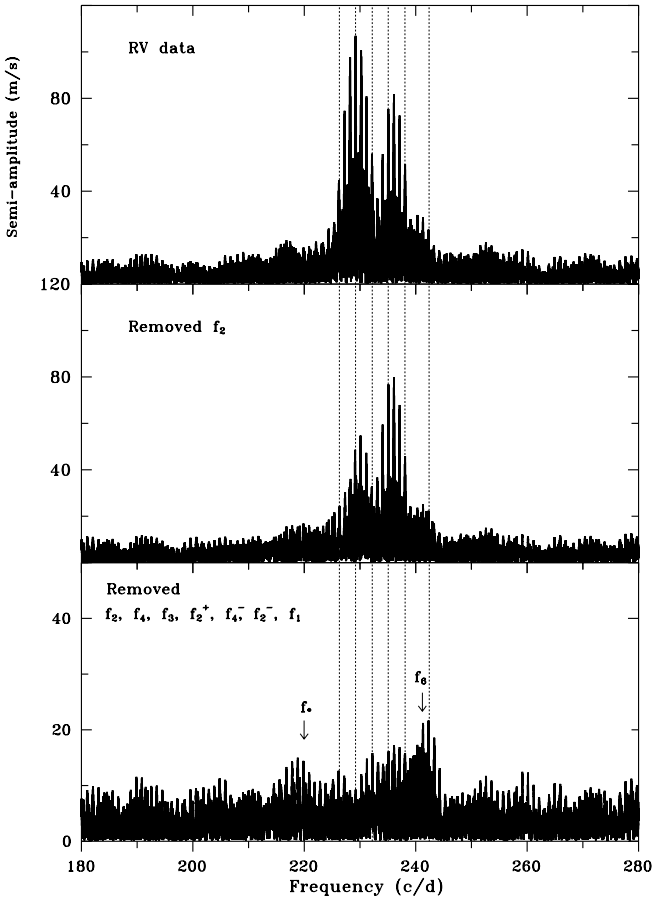

Fig. 6. The amplitude spectra of consecutive steps of a DFT analysis for the entire RV data. The position of principal frequencies from Kurtz et al. (1989) are indicated by dashed lines. (Top) DFT of original RV data. (Middle) DFT of RV residuals after removing contribution from f_2. (Bottom) DFT of residuals after removing the principal frequencies f_1, f_2, f_4, f_3 and the rotationally split sidelobes f_2^+, f_4^-,f_2, and f_2^-. The f_6 mode (Kurtz et al. 2002) as well as a suspected new mode with amplitude of 14.3 m s^{-1} and frequency of 219.9 ± 1 c d^{-1} (2545.1 μHz) are shown by arrows in the bottom panel.

Second, we undertook this broad-band analysis separately for every night with the aim of studying the rotational variation of the amplitude and phase of individual modes. Finally, as a check of the broad-band results we analyzed the RVs for a single spectral feature, Nd III 5294.1 Å, that showed high pulsational amplitudes. The work on Nd III is a precursor to a complete line-by-line analysis of HR 1217 to published as part of our series in the RV study of roAp stars.

3.2. Analysis of the 5776–5873 Å region

3.2.1. Entire data set analysis

We performed a frequency analysis for the entire dataset of the order centered on 5825 Å (5776–5873 Å) which contained 2075 data points spanning 48 days from the first to the last observation. The top panel of Fig. 6 shows the amplitude spectrum of the HJD 2 450 798–2 450 846 RV data. (For convenience we will refer to the data from each night by the integer value of the Julian Day for that night.) Pulsation

Table 2. Photometric frequencies f_1-f_7 detected in analysis of entire data of the spectral order centered on 5825 Å. Also listed are the new modes detected in different subsets of the RV data.

No.	Frequency		K	σ_K
	c d^{-1}	μHz	m s^{-1}	
Analysis of entire data set of λ 5825Å order				
f_1	226.324	2619.5	20.1 (var)	±0.6
f_2^-	229.151	2652.2	18.6	±0.7
f_2	229.206	2652.9	114.4 (var)	±0.6
f_2^+	229.294	2653.9	33.7	±0.7
f_3	232.135	2687.6	53.9 (var)	±0.6
f_4	235.090	2720.9	88.4 (var)	±0.6
f_4^-	234.992	2719.8	37.3	±0.7
f_6	241.29	2792.7	19.6 (var)	±0.7
Analysis of subsets of the λ 5825 Å spectral order				
f_5	238.09	2755.7	40.3 (var)	±0.7
f_7	242.41	2805.7	53.4 (var)	±0.7
Analysis of subsets of the Nd III 5294.1 Å line				
f_{-1}	220.58	2553.0	59.9 (var)	±0.7
f_0	223.37	2585.3	50.3 (var)	±0.7

frequencies were found using the following pre-whitening procedure. A sine wave was fit to the dominant frequency and this component was removed from the data. An analysis was then performed on the pre-whitened data and the contribution of the next dominant mode was then removed. The steps of this analysis are shown in the top and middle panels of the figure. Through this sequential pre-whitening procedure we were able to find the principal photometric frequencies with their sidelobes: f_2, f_4, f_3, f_2^+, f_4^-, f_2^- and f_1, where the symbols $^+$ or $^-$ denote the rotational sidelobes (f + $f_{\rm rot}$ and $-f_{\rm rot}$) The bottom panel of Fig. 6 shows the DFT of the RV residuals. The highest and approximately equal strength peaks occur at frequencies of 241.29 and 242.29 c d^{-1} and have amplitudes of 21.3 m s^{-1} and 21.6 m s^{-1}, respectively. The second frequency is clearly a 1 c d^{-1} alias of first. The 241.29 c d^{-1} (2792.7 μHz) peak coincides with the mean position of the new f_6 mode and is close to the f_7 mode. These two modes could not be safely resolved by our RV data due to their close spacing and the 1 c d^{-1} pattern in the spectral window function.

There is also excess power above the 12 m s^{-1} noise level (at surrounding frequencies) in the interval 219–220 c d^{-1} and 232–238 c d^{-1}. In the interval 232–238 c d^{-1} this excess may be naturally explained by a combination of the small-amplitude f_5 mode and its unresolved, rotationally split sidelobes, along with the residual sidelobes of f_4 and f_3. Because further attempts to resolve the low-amplitude sidelobes in the interval 229–238 c d^{-1} could not provide additional information we focus on the frequency interval centered around 220 c d^{-1}.

The RV noise peaks of our broad-band radial velocity data for the entire data set is about 12 m s^{-1} in the frequency range of interest. This leads us to suspect that the signal around frequency = 220 c d^{-1} is indeed real. To show that this signal is

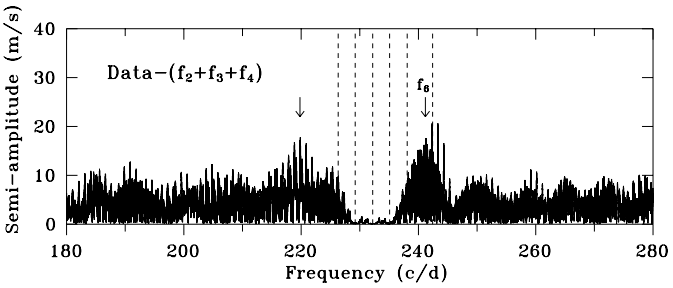

Fig. 7. The amplitude DFT spectra of merged nightly residuals after removing the contribution of f_2, f_3, and f_4 determined by least squares solutions for every night. The position of the principal frequencies from Kurtz et al. (1989) are indicated by dashed lines. The right arrow (f_6) marks the location of the most recent photometric mode (Kurtz et al. 2002) and the f_7 mode is the dashed line to its immediate right. The new suspected mode is shown by the arrow to the left.

not an artifact we analysed the broad-band data in another way. First, for every night we approximated the signal from the contribution of high amplitude f_2, f_3, and f_4 modes using the simultaneous least square sine wave solution with fixed frequencies, but with variable phases and amplitudes. We removed this three-frequency fit from the RV measurements of each night. This procedure automatically removed the rotation sidelobes of the large amplitude modes from the DFT of the data from the combined nights which simplified the search for new low-amplitude modes. We merged all the nightly residuals into the one residual data set for a further search for periodicities. The DFT analysis of this data set is shown in Fig. 7 and this gives approximately the same result as the consecutive prewhitening procedure for the entire data set. The right arrow in the figure marks the location of f_6 and the left arrow the new suspected mode with a frequency = 219.9 ± 1 c d^{-1} (2545.1 μHz) and an amplitude = 17.8 m s^{-1}. The ± 1 c d^{-1} uncertainty is due to alias pattern of spectral window function. This is consistent with the consecutive pre-whitening procedure of the previous analysis.

The statistical significance of the two peaks in Fig. 7 (indicated by arrows) was assessed using a bootstrap randomization technique (e.g. Murdoch et al. 1993; Kürster et al. 1997). The measured RV values were randomly shuffled keeping the observed times fixed. A Lomb-Scargle periodogram (Lomb 1976; Scargle 1982) was then computed for each shuffled data set. The fraction of the random-data periodograms having peak power greater than the observed peak power in the frequency interval $190 < \nu < 260$ c d^{-1} was taken as the false alarm probability (FAP) that random noise could produce the observed signal. We should note that this is a very conservative estimate for the FAP of signals known to be present in the data (like f_6 which has been found photometrically). In this case one should determine the probability that random noise produces a peak higher than the data periodogram at *exactly* this frequency and not over the broad frequency range that we considered.

Using 10^5 "shuffles" we determined FAP = 8.6×10^{-5} for f_6 and FAP = 9.5×10^{-3} for the peak at 219.9 c d^{-1} (2545.1 μHz, termed f_0). The detection of f_6 is highly significant and thus provides spectroscopic confirmation of this new photometric mode. The detection of f_0 is marginally significant. (Our criterion for a statistically significant signal in the data is that it must have FAP $< 10^{-3}$). However, in the next subsection we show that based on a single night analysis this signal is most likely real and due to an additional excited mode.

The analysis of whole data set shows that the all principal photometric frequencies known for HR 1217 (Kurtz et al. 2002) are also present in our high precision RV data, but the RV amplitude ratios of the modes do not follow the photometric amplitude ratios. For instance, the highest RV amplitude in our observations is at 229.21 c d^{-1} (2652.9 μHz = f_2) whereas the highest photometric amplitude was reported in 1986 at 232.2 c d^{-1} (2687.5 μHz = f_3, Kurtz et al. 1989), and 235.08 c d^{-1} (2720.8 μHz = f_4) using data taken in 2000 during a *Whole Earth Telescope* campaign (Kurtz et al. 2002). The differences in photometric amplitudes could be explained by temporal amplitude variability. A different RV-to-photometric amplitude ratio of modes is also consistent with suggestion that different acoustic modes will have different phase and amplitude profiles across the atmosphere (Mkrtichian et al. 2003) and hence results in different amplitudes in the continuum and line-forming layers.

3.2.2. The nightly amplitude and phase analysis

The analysis of all the data distributed over the whole rotation period can provide higher frequency resolution, but leads to loss of information regarding the shape of variability of the pulsational amplitudes and phases over a rotation cycle.

Knowing the exact photometric frequencies for modes will enable us to investigate the night-to-night amplitude and phase variability in RVs. Moreover, this analysis for the separate nights will help us to determine the nights with nearly constant pulsational phases. This will allow us to combine these into one data string in order to obtain a higher frequency resolution and a better signal-to-noise ratio for detecting low amplitude signals.

A least squares fit to a single night of observations using seven fixed frequencies, but with variable amplitudes and phases may in some cases give unrealistic and divergent solutions. We thus chose to fit the data from the individual nights simultaneously with the frequencies of two highest amplitude modes (usually f_2 and f_4). The contribution of these were then subtracted and a simultaneous one- or two-frequency solution was performed on the residuals using the known (fixed) values of photometric frequencies. Such a technique helps to avoid uncertain results that may arise during the multi-frequency fitting of a short time series of data.

Figure 8 shows the DFT of the nightly RV data using the spectral order centered on 5825 Å. Figure 9 shows a phase plot of the residual RVs after removing a three-frequency fit (f_2, f_4, and f_5) to the data taken on JD 2 450 804 and phased to the remaining best fit frequency 241.7 c d^{-1} (2797.5 μHz). This signal is most likely a doublet of two close frequencies (f_6 and f_7) and has a semi-amplitude 56.2 m s^{-1}.

This procedure was then performed on data from all nights to find the multi-frequency amplitude and phase solutions for

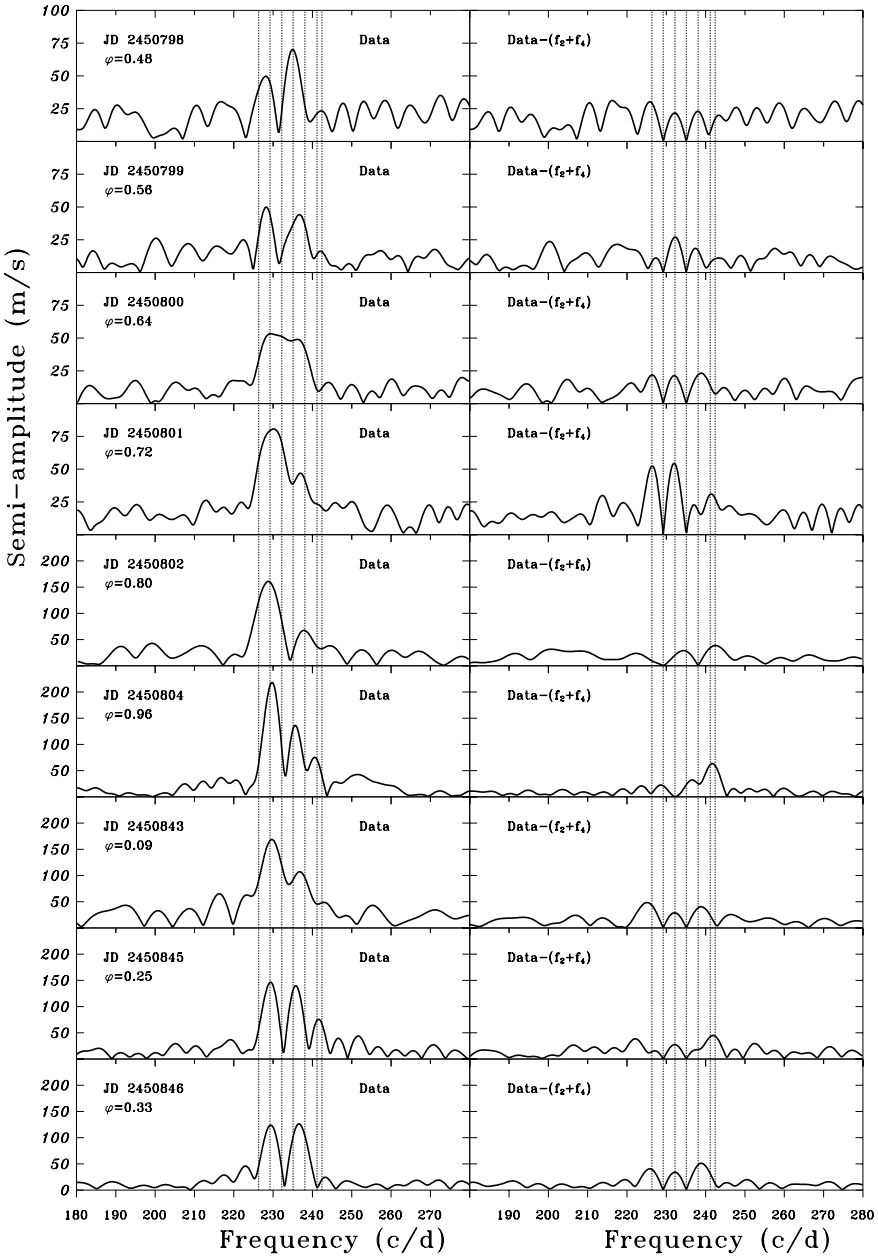

Fig. 8. DFT of the "broad-band" RVs of the order centered on 5825 Å from the individual nights (*left panels*, *from top to bottom*) and after subtracting a two-frequency solution (*right panels, from top to bottom*). Note the different RV scale for the upper four panels. The vertical dashed lines shows the position of the photometric frequencies from Kurtz et al. (2002). The Julian dates and the corresponding mean rotation phases are given for each panel.

residuals as a function of rotation phase. We also checked some multi-frequency solutions that were uncertain by combining two consecutive nights for the DFT analysis and comparing these to results using only one night of data. The resulting rotational amplitude and phase variability of the highest amplitude modes (f_2, f_3 and f_4) is presented in panels of Fig. 10. These will be discussed in Sect. 4.1.

On the night of JD 2 450 845 (ϕ = 0.25) the residual DFT (see the right panel of Fig. 8) showed significant power (amplitude of 40 m s^{-1}) at 222.1 c d^{-1} (2570.6 μHz). This confirms our suspicion (see above) regarding the presence of additional modes excited with frequencies between 220–223 c d^{-1}.

3.3. The Nd III 5294.1 Å RV analysis

To check the results of the previous subsections, we analysed the RV measurements of a single spectral line, the strong feature of Nd III at 5294 Å which was found to have a high RV amplitude. Data were analyzed from several nights centered on the selected rotation phases that did not show significant pulsation phase and amplitude variations for f_2 and f_4. (This facilitates correctly subtracting the contribution of these modes.) The f_2 mode had its maximum RV amplitude of 322.9 m s^{-1} on the night JD = 2 450 804. A short time series of the RV measurements for this Nd III spectral line is shown in Fig. 11. An analysis of this night showed that the signal around 220 c d^{-1} was not detectable (possibly due to rotational modulation).

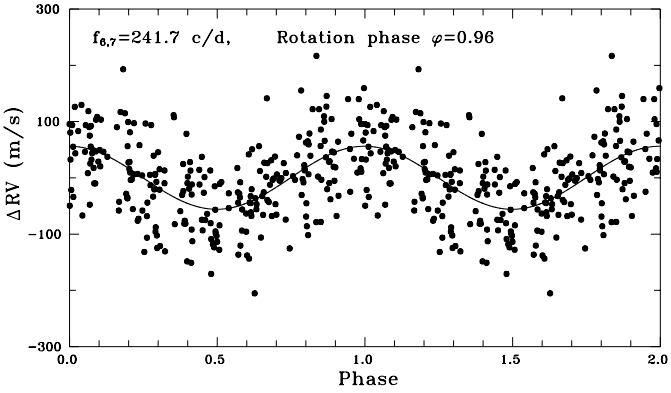

Fig. 9. The phase curve of residuals after removal of a three frequency fit (f_2, f_4 and f_5) to data from the night JD 2 450 804. This is phased to the best fit frequency fit of 241.7 c d^{-1} (exactly between f_6 and f_7). The semi-amplitude of remaining two mode pulsations is 56.2 m s^{-1}. Data points are repeated for the second cycle.

We then analysed the RVs of the Nd III 5294.1 Å line from on JD = 2 450 845. Figure 12 (top panel) is the DFT of the original data. The bottom panel show the DFT of residuals after subtracting the fit to the f_2 from the data. This shows a signal with amplitude = 76 m^{-1} at a frequency of 221.39 c d^{-1} – approximately midway between the 220.4 and 223.3 c d^{-1} modes expected from equally spaced p-modes in HR 1217. This is probably an unresolved blend of these frequencies. The FAP of this peak using the bootstrap randomization technique and 2×10^5 shuffles is FAP $< 5 \times 10^{-6}$. This is statistically significant and confirms that the signal found in broad-band RV analysis at frequencies shorter than f_1 mode is indeed real. Figure 13 shows the RV residuals phased to a period of 6.477 min (ν = 222.33 c d^{-1} = 2573.3 μHz). Each point represents phased-averaged measurements using a bin size of 0.05 pulsation phases.

To check independently this detection and to resolve the blended peaks by extending the time-base, we performed a DFT analysis on two closely-spaced nights JD 2 450 843 and 2 450 845 that covered the rotation phases ϕ = 0.09–0.25. This corresponds to the relatively stationary pulsation phase of f_2 and f_4 modes (i.e. no jumps in the pulsational phase occur from one night to the next).

The signals of the highest amplitude modes (f_2 and f_4) were pre-whitened from the nightly data and the residuals were merged into one data set for analysis. The top panel of Fig. 14 shows the DFT of these residuals with two resolved peaks: f_{-1} at ν = 220.58 c d^{-1} = 2553.0 μHz (K_{-1} = 59.2 m s^{-1}) and f_0 at ν = 223.37 c d^{-1} = 2585.3 μHz (K_0 = 50.3 m s^{-1}). The f_{-1} peak is statistically significant having FAP = 6.5×10^{-5} determined by 10^5 runs of a bootstrap randomization scheme. The bottom panel of Fig. 14 shows the DFT of residuals after the pre-whitening the f_{-1} signal. The FAP of the f_{-0} peak is 7.2×10^{-4}. The remaining low amplitude peaks in the 220–243 c d^{-1} interval corresponds to the f_3 and f_5 modes.

One more statistically significant new peak (having the broad alias sidelobes) in the DFT is at a frequency 244.07 c d^{-1} (2824.9 μHz). This has a maximum amplitude of 52.8 m s^{-1} and a FAP = 2.0×10^{-4} (10^5 shuffles). The frequency of this peak (which is probably a blend with the f_7 = 242.4 c d^{-1} (2805.6 μHz) mode) is exactly at the expected position (f_8 = 244.2 c d^{-1}) of the next equally spaced (with f_6) mode. However, it is a premature to conclude, based on quality of available subset of RV data, about the existence of new excited mode outside the interval of 220–243 c d^{-1}.

As a final check of the certainty of the detection of the two new modes in the interval 220–223 c d^{-1} we carried out an analysis of another subset of ND III 5294.1 Å line RV data, namely those taken on the consecutive nights JD = 2 450 800 and 2 450 801. These nights correspond to another rotation phase interval (ϕ = 0.64–0.72) with relatively constant (after π-switching) pulsation phases for f_2, f_3, and f_4. Figure 15 shows the DFTs of raw data and the residual RVs after application of the consecutive pre-whitening procedure on the two highest amplitude peaks of f_2 and f_4. The residual DFT (bottom panel) shows a pattern of peaks with amplitudes around 30 m s^{-1} at the positions of the f_1, f_3, f_6 and f_7 modes. A peak at 221.5 c d^{-1} (2563.7 μHz) is exactly the position of the 1 c d^{-1} alias of 220.4 c d^{-1} (2550.9 μHz, marked as f_{-1}) which follows the equidistant spacing of the f_0–f_6 sequence. The FAP of this peak is 9.1×10^{-3}. We do not see f_0 frequency which is most likely a result of rotational modulation of the pulsational amplitude.

In summary, our analysis confirms the existence of the new photometric f_6 mode. We have detected with a high statistical significance two new pulsation frequencies, 220.58 c d^{-1} (2553.0 μHz) and 223.37 c d^{-1} (2585.3 μHz), using RV measurements from subsets of our "broad-band" spectral data and from a single spectral line (Nd III 5294.1 Å). These follow the f_1–f_6 equidistant spacing i.e. related to the same odd and even l-degree sequences of p-modes.

4. Discussion

4.1. The rotational amplitude and phase variability

The expected effect of a large global magnetic field is to modify the pure zonal mode of pulsation giving rise to magnetically perturbed components (Takata & Shibahashi 1995; Dziembowski & Goode 1996). The revised oblique pulsator model that includes the effects of the centrifugal force and the magnetic field was suggested by Bigot & Dziembowski (2002). For a dipole mode they developed a simple geometrical picture of non-axisymmetric pulsations in the presence of rotation and magnetic field that explained the observed pulsational amplitude modulation. This two-dimensional model is valid for polar magnetic field strengths greater than 1 kG and needs to be established by observations.

Recently, excitation of axisymmetric non-radial p-modes in the presence of a magnetic field was investigated by Saio & Gautschy (2004). They show that only high-overtone modes excited by classical κ-mechanism survive in the presence of a few kG magnetic field and the amplitudes of the mainly dipole or quadrupole modes are strongly confined to the magnetic axis. The comparison of observed rotational RV modulation for different modes with those predicted by different pulsator models may be a valuable tool for checking which model is correct.

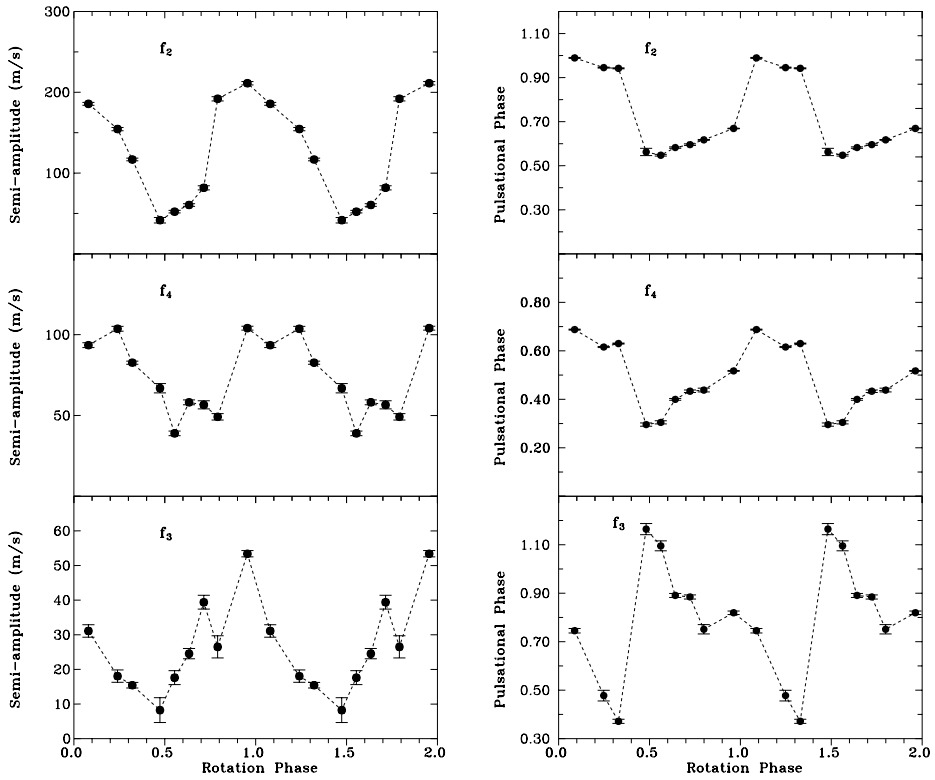

Fig. 10. Pulsation amplitude and phase for the f_2, f_3 and f_4 modes as a function of rotation phase. Note the different amplitude scales for different modes. Data points are repeated for the second cycle.

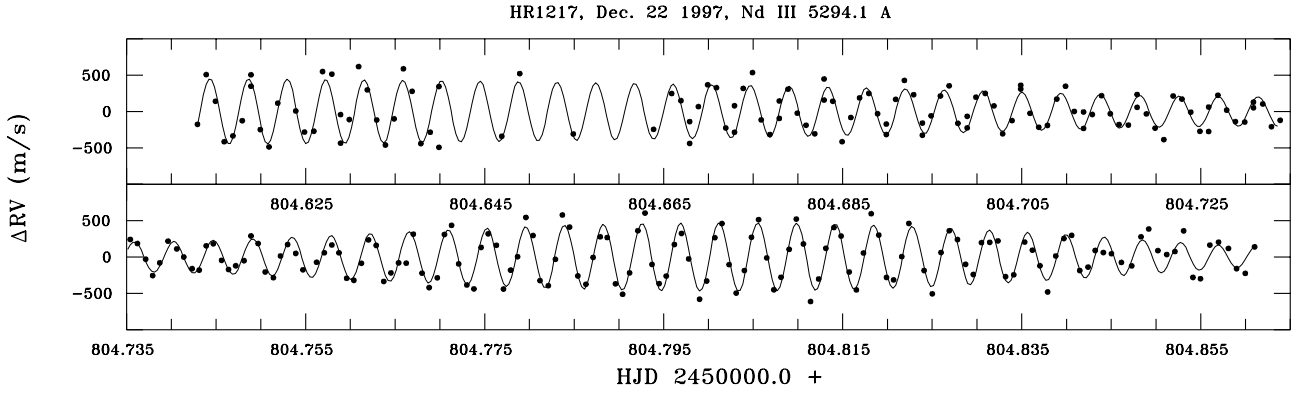

Fig. 11. The pulsation RV variations of the Nd III 5294.1 Å spectral line obtained on JD 2 450 804.

We compared the observed and predicted pulsational amplitude variations for HR 1217 for l = 1–3 zonal (m = 0) modes in the context of the standard 2D-OPM model. This was done using the SPOTNRP code (Mkrtichian 1992) written for modeling line-profile variations and the spatial response functions for 2D-OPM in roAp stars with surface chemical anomalies. Our simulations were carried out for the low-degree l = 1–3, m = 0 modes that covered the complete rotational period of HR 1217. Figure 16 shows the variations of the modulus of the disc-integrated amplitudes for these modes normalized by the maximum surface velocity amplitude. We assumed no surface anomalies for these calculations in order to compare to the results of our analysis of the 5825 Å spectral order which represents an average RV of many spectral lines from a variety of atomic species. The effect of the surface inhomogeneous distribution of elements investigated by Mkrtichian (1994) and Mkrtichian et al. (2000) should thus be nearly eliminated. In the oblique pulsator model for HR 1217 we assume inclination angles for the rotation and magnetic axes of $i = 140 \pm 5°$, $\beta = 147 \pm 5°$, respectively, as determined from the linear polarization data of Leroy et al. (1996).

The amplitude and pulsation variations for the three high amplitude modes f_2, f_3, and f_4 are shown in Fig. 10. The comparison of Figs. 16 with 10 shows that the shape of the amplitude modulations for the f_2, f_4, modes are close to that expected from a zonal l = 1 mode having its highest amplitude at magnetic maximum. These show a maximum amplitude centered

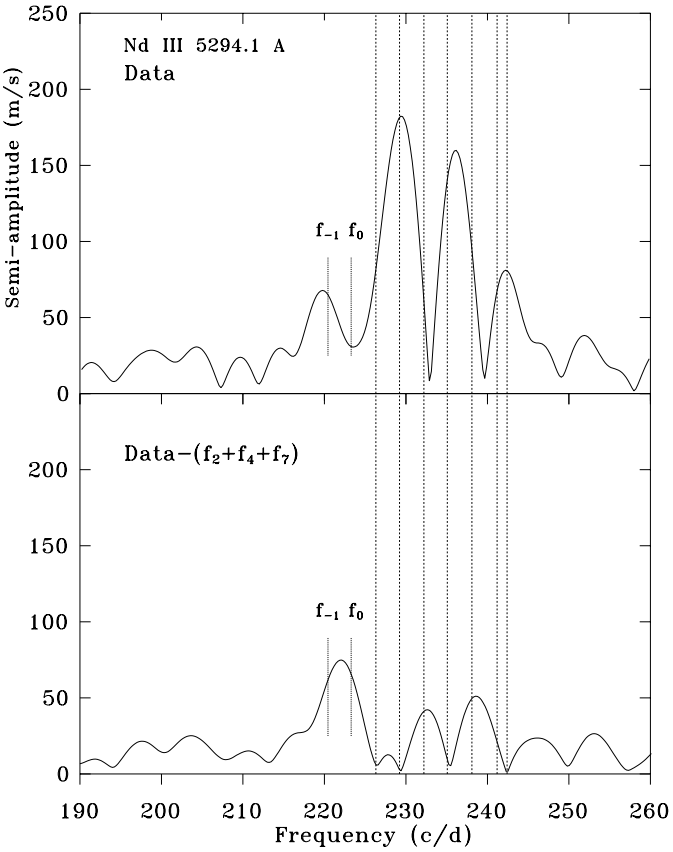

Fig. 12. The frequency analysis of the RV measurements of the Nd III 5294.1 Å line obtained on JD 2 450 845. (*Top panel*) The DFT of original RV data. (*Bottom panel*) The DFT of the residual RV data after subtracting the contribution due to f_2 ($K_2 = 163.25$ m s^{-1}), f_4 ($K_4 = 112.81$ m s^{-1}), and f_7 ($K_7 = 64.04$ m s^{-1}). The long vertical dashed lines show the position of all seven known photometric frequencies in the range of 226–242 c d^{-1}. The two short vertical lines show the expected equally spaced position of new p-modes at frequencies 223.3 c d^{-1} and 220.4 c d^{-1}. Note the strong blended peak ($K = 76$ m s^{-1}) located approximately between these new frequencies.

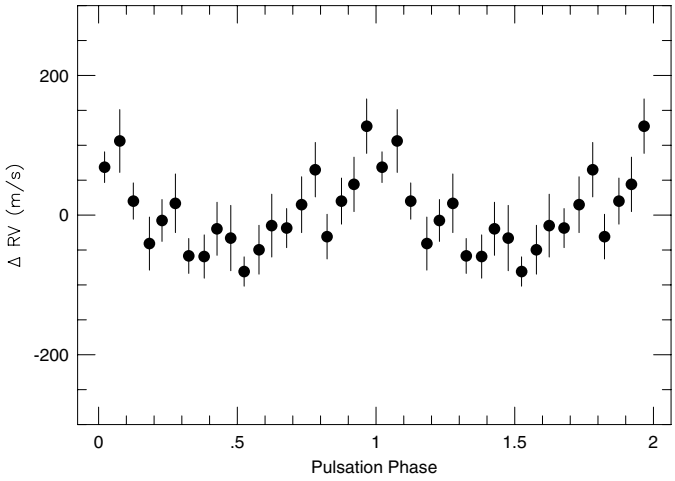

Fig. 13. The phase curve of JD 2 450 845 RV residuals after removing the contribution due to f_2, f_3, f_4, f_5, and f_7. The residual RV measurements are phased with a new, best fit frequency of 222.33 c d^{-1} ($K = 66.3$ m s^{-1}) which is located between frequencies f_{-1} and f_0 and is likely the blend of these two modes. Phases are reckoned from the time of RV maximum. The data are binned into intervals 0.05 of pulsation period and are repeated for the second cycle.

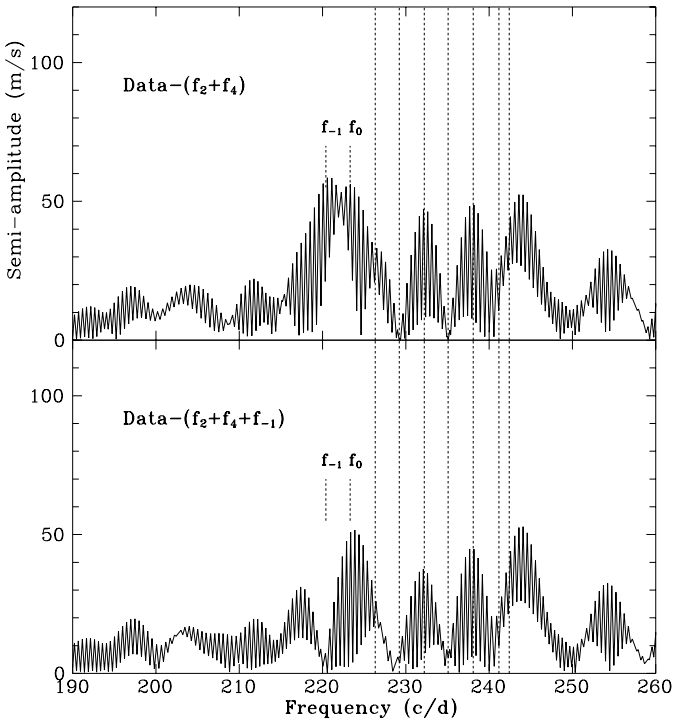

Fig. 14. The amplitude spectra for two merged residual RV data of the Nd III 5294.1 Å line from the nights JD 2 450 843 and 2 450 845. This residual data results from two consecutive steps of pre-whitening the data by the contribution of f_2 and f_4. The long vertical dashed lines show the positions of the seven known photometric frequencies. The two short dashed vertical lines at 223.3 c d^{-1} (marked as f_0) and 220.4 c d^{-1} (marked as f_{-1}) show the expected positions of the two modes extrapolated from the equidistant spacing of the f_1–f_6 series. The well resolved peaks at frequencies of 220.58 ± 0.03 c d^{-1} ($K_{-1} = 59.9$ m s^{-1}) and 223.37 ± 0.03 c d^{-1} ($K_0 = 50.3$ m s^{-1}) correspond to new detected modes.

on rotation phase $\phi = 1.0$ and a minimum around $\phi = 0.5$. Since magnetic maximum occurs at $\phi = 1.0$ this is consistent with the 2D-OPM.

On the other hand, the rotational modulation of the pulsational phase of the f_2, f_4 and f_3 modes does not seem to be consistent with any mode in the standard 2D-OPM. The f_2 mode shows a pulsational phase jump exactly at magnetic maximum while the f_4 and f_3 modes show a relatively monotonous change in phase (see Fig. 10) around the rotation phase coincident with the magnetic maximum.

The results of our modeling shown in Fig. 16 demonstrate that for pulsations aligned with the magnetic axis the $l, m = 1, 0$ mode does not show pulsational phase jumps, only the zonal modes $l = 2$, 3 have approximately a π phase jump (hereafter "π-switching") during the rotation cycle. The pulsation phase for HR 1217, according to the 2D-OPM, should be switched at $\phi \simeq 0.28$ and $\phi \simeq 0.72$ for $l = 2$ modes, and at $\phi \simeq 0.19$ and $\phi \simeq 0.81$ for $l = 3$ modes (see Fig. 16). However, all $l = 1$–3

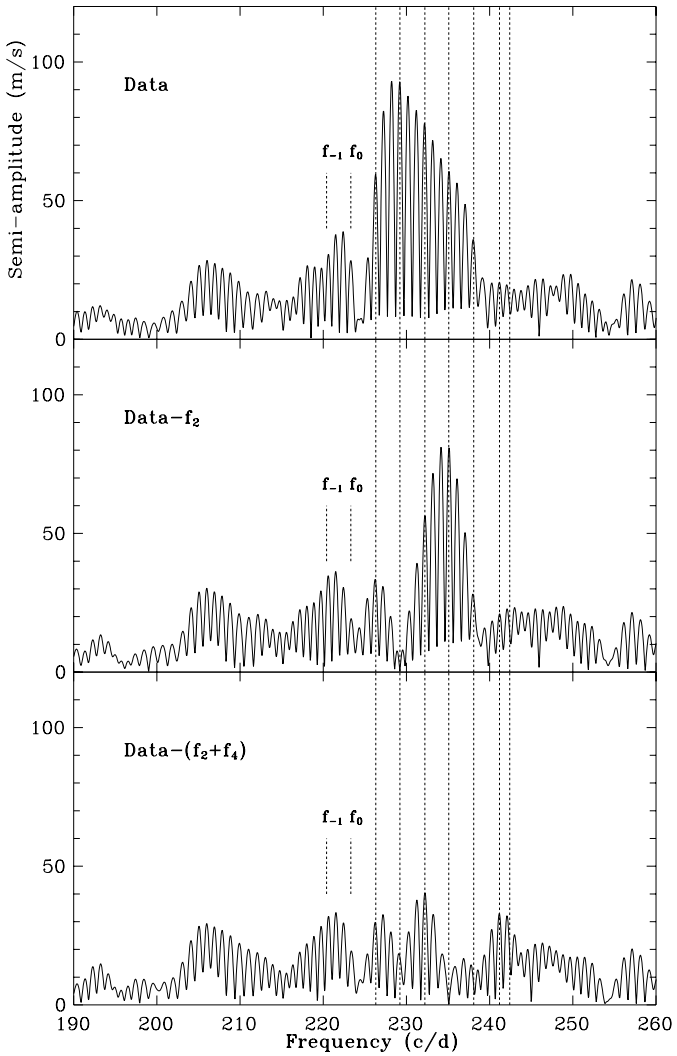

Fig. 15. DFT analysis of combined data for Nd III 5294.1 Å spanning JD 2 450 800–2 450 801. (*Top*) DFT of the original data. (*Middle*) DFT of the residuals after pre-whitening by the f_2 mode. (*Bottom*) DFT of the RV residuals after prewhitening by the f_2 and f_4 ($K_4 = 80.0\,\mathrm{m\,s^{-1}}$) modes. The remaining peaks correspond to f_1 ($K_1 = 30.0\,\mathrm{m\,s^{-1}}$), f_3 ($K_3 = 40.3\,\mathrm{m\,s^{-1}}$), and f_6 ($K_6 = 30.0\,\mathrm{m\,s^{-1}}$). The short vertical lines show the expected positions (at $223.3\,\mathrm{c\,d^{-1}}$ and $220.4\,\mathrm{c\,d^{-1}}$) of two modes extrapolated from the f_1–f_6 equidistant mode spacing. Note the missing signal of the f_0 mode that is a indication of rotational modulation of this mode.

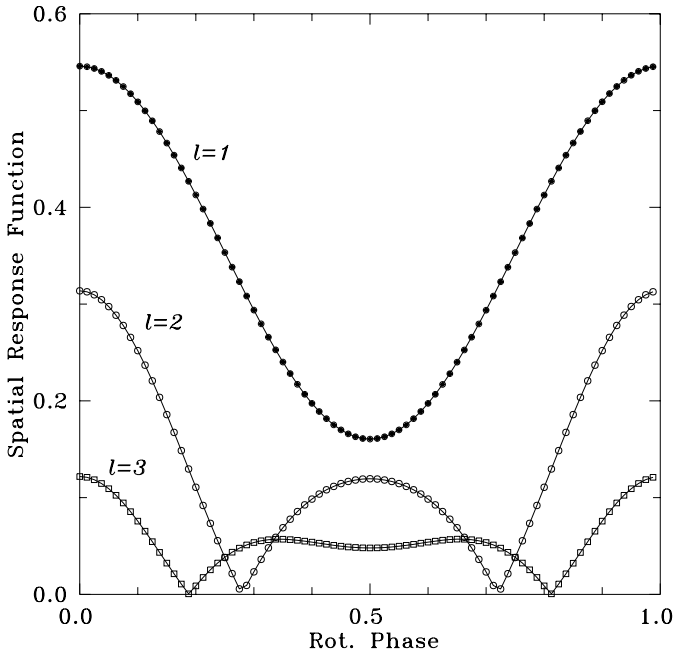

Fig. 16. The calculated rotational modulation of the relative RV amplitudes (modulus of the spatial response function) of pure $l = 1$, 2 and 3 zonal ($m = 0$) modes in a standard OPM for HR 1217. The pulsation phase is positive around the magnetic maximum ($\phi = 1.0$) and switches sign after every pass of the response function through zero. The $l = 1$, $m = 0$ mode does not change its pulsation phase over the rotation period reflecting the non-reversive variations of magnetic field in HR 1217.

pure zonal modes cannot explain the observed variability and phase jumps of f_2, f_3, and f_4 in HR 1217.

The pulsation phase "π-switching" for the f_2 mode occurs exactly at magnetic and pulsation amplitude maxima, i.e. between rotation phases $\phi = 0.96$ and 0.09, and then jumps back at rotation phases 0.33–0.48. This is inconsistent with what is expected from the standard 2D-OPM. For the f_4 and f_3 modes the phase variations are different with respect to the f_2 mode. The pulsational phase for both modes jumps at $\phi = 0.33$–0.48. Over the rotational phase interval $\phi = 0.48$–1.33 the pulsation phase of f_3 decreases while the phase of f_4 increases almost linearly back to its previous values. It is during this phase interval that the magnetic pole crosses the line-of-sight. The interpretation of the phases for f_2, f_4 and f_3 in terms of any pure $l = 1$, 2 or 3 zonal mode and the standard 2D-OPM thus encounters problems.

An attempt to decompose the observed RV phase jumps and amplitude modulation around the magnetic maximum for the f_2 and f_4 modes by a linear combination of correspondingly scaled spherical harmonics can be productive if there is some realistic theoretical predictions about the limits for a range of (l, m) quantum numbers in the expansion. According to Dziembowski & Goode (1996) and Cunha & Gough (2000) magnetically perturbed l-degree eigenmodes will have strong $l \pm 2$ components in their expansions and could be misidentified with each other. The original $(l, m) = (2, 0)$ modes may have a strong $l = 0$ and $(l, m) = (4, 0)$ components, whereas the $(l, m) = (1, 0)$ mode will have $(l, m) = (3, 0)$ components. Conversely, the $(l, m) = (3, 0)$ modes have strong $(l, m) = (1, 0)$ and $(l, m) = (5, 0)$ components. So, the modes of even and odd degrees are expected to have odd and even terms in the expansion.

However, it is clear from Fig. 10 that the phase jump in f_2 at magnetic maximum is not possible to represent as a combination axisymmetric $m = 0$ modes because all amplitude and phase changes of $l = 1$–4 zonal modes are symmetric with respect to the magnetic maximum. There are difficulties if one attempts to explain the phase changes between $\phi = 0.48$ and 1.33 using a linear combinations of magnetically distorted zonal l-components for the f_3 and f_4 modes since during this time the magnetic pole crosses the line of sight.

It might seem that for the interpretation of the RV phase variability in the HR 1217 it will be better to include the non-axisymmetric components in distorted pulsations expansions as suggested by Takata & Shibahashi (1995) or as proposed by the revised OPM of Bigot & Dziembowski (2002). Again it is difficult to adjust simultaneously within the framework of the 2D-OPM model the maximum of pulsation RV amplitude and the RV phase switching and the constancy of the photometric phase around the magnetic maximum.

In retrospect, Mkrtichian et al. (2000) showed (see Figs. 3 and 4 in their paper) that the spotted distributions of chemical elements in a standard 2D-OPM model may produce additional modulation of the RV pulsation amplitudes for lines of individual elements. These may introduce shifts in the rotational phase where the pulsational π-switching occurs while the photometric phase might show no anomalies. The magnitude of this effect for every mode depends on the abundance, geometry, and location of spots on the stellar disk with respect to pulsation axis. At some favorable inclinations of the magnetic axis the contribution of the surface spots may saturate the π-switching of pulsation phases for magnetically reversive roAp stars. In turn, for some favourable geometry of spots and inclinations of magnetic, rotation and pulsations axes, this effect may lead to π-switching of phases in the RV even for roAp stars that do not show (like HR 1217) magnetic field reversals and pulsation phase π-switching in the photometry. However, the similarities in π-switching in the "broad-band" RV phases at magnetic maximum in HR 1217 is seen to occur in the f_2 mode (see Fig. 5) and in all spectral orders covering the wavelength range 5010–6300 Å. These regions include several tens of spectral lines from many different chemical elements; any effects due to abundance spots on the stellar surface will thus average out. In the case of the f_2, f_3, and f_4 modes we therefore cannot invoke abundance spots as a main cause of the peculiar rotational phase variations observed in HR 1217. The observed phase variations are inconsistent with those predicted by the standard or modified 2D-OPM. The origin of the phase variations must have another physical nature.

The picture of atmospheric pulsation velocity amplitudes and phases in roAp stars, as follows from recent spectroscopic results (Kanaan & Hatzes 1998; Baldry & Bedding 2000; Mkrtichian et al. 2003; Kurtz et al. 2003), is more complicated. Mkrtichian et al. (2003) using the new technique of acoustic cross-sections found the existence of standing wave and running wave components in RV variations and oppositely pulsating layers in the atmosphere of 33 Librae. The hypothetical standing wave likely has two acoustic nodes – one close to continuum formation level and another in the superficial atmospheric layers. They predicted that the acoustic profiles across the atmosphere should be different for different modes. Independently, Kurtz et al. (2003) using the VLT spectroscopy found evidence of running wave component in the upper atmosphere of the roAp star HD 166473.

Any attempt to give a reasonable explanation of the rotational RV phase and amplitude variability in HR 1217, or any other roAp stars, should also reflect the existence of vertical acoustic waves and nodes in atmosphere. Such complicated atmospheric vertical amplitude and phase acoustic profiles should lead also to strong line-profile variations especially in the case of vertical stratifications of elements. In this case, during a pulsation cycle, the layers contributing to the wings and core of spectral lines may have opposite velocity shifts and these can introduce strong line-profile variations even for slowly rotating roAp star. In the framework of two-dimensional models of non-radial pulsations, such line-profile variations can be mis-interpreted as a non-axisymmetric sectoral or tesseral mode oscillations as was suggested for the line-profile variations in γ Equ (Kochukhov & Ryabchikova 2001a).

In this sense, the 2D-OPM should be revised and we should consider a three-dimensional oblique pulsation model (3D-OPM). That is, a pulsational phase and amplitude that is a function of location on the stellar surface *and* depth in the stellar atmosphere. This picture would be consistent with the observed photometric and RV variations in HR 1217. An attempt to understand such a 3D-OPM and detailed analysis of observed line-by-line RV amplitude and phase variations in HR 1217 is beyond the scope of the current work and should be given in detail in one of the next papers on our series on RV studies of roAp stars.

4.2. P-mode spacing and the problem of the f_7 mode

In this paper we found that the p-mode oscillation spectrum for HR 1217 derived from RV measurements is consistent to the photometrically determined one. Two new frequencies were also found with a frequency spacing $\approx 34\ \mu$Hz. This frequency spacing in HR 1217 was explained by Shibahashi (1984) as half the value $\Delta\nu_0/2$ for consecutive overtones, and that the observed frequencies are due to alternative odd and even l-modes with a principal spacing $\Delta\nu_0 = 68\ \mu$Hz. The only frequency which did not follow to this interpretation is $f_7 = 242.4\,\mathrm{c\,d^{-1}}$ ($2806.4\,\mu$Hz). The discovery of the peculiar spacing of the $2806.4\,\mu$Hz mode (Kurtz et al. 1989) has led to discussions on its nature. A recent review summarizing this problem can be found in Cunha (2001).

For completeness, we will give another possible, but simple explanation of the non-equidistant spacing. We would like to stress that all previous explanations of the f_7 mode and its probable breaking of the equidistance spacing of modes (Kurtz et al. 1989; Cunha 2001) were made under two assumptions: *i) that higher degree ($l > 3$-degree) are not detectable, and ii) that the f_7 mode belongs to the same (l, m, n) sequences of odd and even l-degree modes which formed f_1–f_6 equally spaced modes.* However, these widely accepted assumptions about the photometric "invisibility" of high-degree modes due to surface cancellation effect while correct for normal stars, may be not valid in the case of roAp stars. Moreover, low-degree components of magnetically distorted high-degree modes (Dziembowski & Goode 1996) may indeed be visible in disk-integrated light. In photometric studies of roAp stars, the (probably) excited *high-degree modes or their magnetically distorted low degree components, may introduce a significant contribution to the disk-integrated photometric variability and hence may be indeed be detectable in disk-integrated measurements.* This may be due to the peculiar abundances and their inhomogeneous distribution on the stellar surface which can affect the local opacity, and

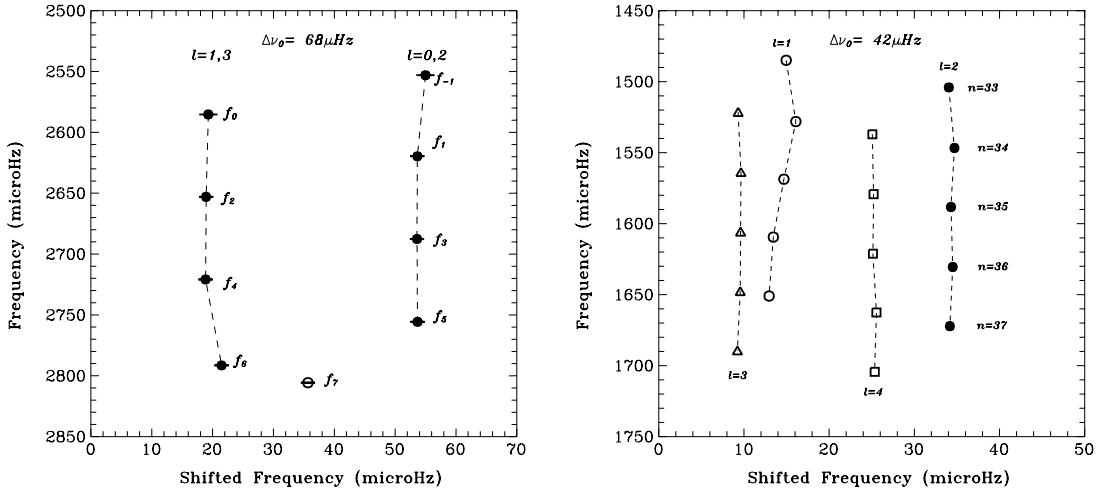

Fig. 17. *Left panel*: p-mode echelle-spectrum of HR 1217. The f_{-1}, f_1, f_3, f_5 and f_0, f_2, f_4, f_6 modes which are likely related respectively to odd and even l-degrees are spaced on ≈34 μHz. The f_7 mode is shown by open circle. *Right panel*: the theoretical l = 1–4 p-mode echelle-spectrum model "L" from Gautschy et al. (1998). The modes with n = 33 to n = 37 and different l-degrees form vertical columns (different symbols). The column representing the l = 4 modes between the l = 1, 3 and l = 2 columns is similar to spacing that is observed for f_7 mode in HR 1217.

possibly even a peculiar limb-darkening law. For spectroscopic studies, Mkrtichian (1992, 1994) and Mkrtichian et al. (2000) show that the surface chemical inhomogeneities in roAp stars may act as a 2D-PSF for nonradial pulsations and allows us to detect in a slowly rotating stars modes up to $l \simeq$ 10–15.

Mkrtichian & Hatzes (2000), in their discussion on the echelle-diagrams for roAp stars and of HR 1217 in particular, have explained the non-equidistant spacing of 2791 μHz (the former f_6 but the present f_7) mode as related to the higher degree modes which may indeed be visible in the disk-integrated light. This explanation is based on the fact that modes with $l > 3$, their (l, n) frequency pattern should be shifted relative to the columns for l = 0 or 2 and l = 1 or 3 modes in the echelle-diagram. In other words, if the f_7 mode is related to another odd or even l-degree sequence (say l = 4 or l = 5) than the one which are formed by f_1–f_6, then the spacing of f_7 with respect to f_6 mode should not be equal to ≈34 μHz. If true, then we predict another sequence of yet undetected l = 4 modes which should be spaced by 68 μHz from f_7.

To elucidate this interpretation using a graphical form we show in the left panel of Fig. 17 the echelle-diagram for HR 1217 with the complete set of modes so far detected. In the right panel for comparison is the constructed echelle-diagram for the frequencies of l = 1–4, n = 33–37 overtone modes from the theoretical model "L" (M = 1.5 $M_\odot$, $\log L/L_\odot$ = 0.96, $\log g$ = 3.816) of Gautschy et al. (1998). Note, that this model does not represent the theoretical spectrum of HR 1217 and is shown only illustrative purposes. The echelle-diagrams (ED) for high-overtone acoustic modes are constructed by dividing the frequency range where the modes are present on the frequency intervals by the value of the so called "large separation", $\Delta\nu_0$, with the next frequency interval placed below the previous one. An ED constructed in this way has vertical columns, each corresponding to the l quantum numbers of adjacent, consecutive overtone modes that are equi-spaced in frequency. We have used the $\Delta\nu_0$ = 68 μHz for HR 1217, and the value 42 μHz for model "L" from Gautschy et al. (1998) which we give as an example of on ED drawn simultaneously for low and high degree-modes. The latter value, found on the direct spacing of frequencies of consecutive overtones, gives a better approximation for spacing onto the vertical columns for a given range of theoretical frequencies than the value 45.34 μHz given for this model in the Table 1 from Gautschy et al. (1998).

As could be seen on the right panel of Fig. 17 the theoretical echelle-diagram for the l = 4 modes form a vertical column that is spaced between low degree odd (l = 1 or 3) and even (l = 2) columns of consecutive overtone sequences in a manner that is qualitatively similar to the spacing of f_7 mode in the echelle-diagram for HR 1217 (left panel). The spacing between (l, $n-1$) = (4, $n-1$) and the closest (l, n) = (1, n) and (l, n) = (2, n) modes is indeed of order $\Delta\nu_0/4$, but in fact the exact spacing of columns depends on stellar models and frequency range of the analysed modes. The l = 4 identification of the f_7 mode naturally explains the former "peculiar" 49.99 μHz ≃ 3/4 $\Delta\nu_0$ spacing between f_7 and f_5, as well as the 14.72 μ Hz ≃ $\Delta\nu_0/4$ spacing between f_7 and f_6.

5. Conclusions

Our preliminary analysis of subsets of high-precision RV data of HR 1217 from spectral data centered on 5825 Å and Nd III 5294.1 Å results in the detection of two new modes with frequencies of f_{-1} = 220.58 c d^{-1} (2553.0 μHz) and f_0 = 223.37 c d^{-1} (2585.3 μHz) that follow the equidistant spacing with the first six (f_1, f_2, f_3, f_4, f_5, and f_6) photometrically detected modes. The RV amplitude ratios of the modes do not follow the photometric amplitude ratios.

The f_3 and f_4 modes showed obvious discrepancies in the phase variability at rotation phases around magnetic maximum. Here the pulsational phase continuously changed without π-switching. We conclude that the observed pulsational phase changes cannot be explained within the framework of the

2D-OPM which assumes that the amplitudes and phase velocity fields and photometric variations depend only on the stellar magnetic latitude and longitude.

We have constructed the echelle-diagram for p-mode spectrum of HR 1217, we give a new, simple interpretation of the peculiar spacing of f_7 as being related to $l = 4$ modes. We predict the existence of another sequence of modes, yet undetected, that should be equally spaced by $68\,\mu$Hz or $34\,\mu$Hz with respect to f_7.

Acknowledgements. D.E.M. acknowledges his work as a part of research activity of the Astrophysical Research Center for the Structure and Evolution of the Cosmos (ARCSEC) which is supported by the Korean Science and Engineering Foundation. D.E.M. is grateful to Alfred Gautschy for making available his models of roAp star and useful discussions. Part of this work was done under the US Civilian Research and Development Foundation (CRDF) grant UP2-317 and a grant by the German Academic Exchange Service (DAAD). A.P.H. acknowledges the support of grant 50OW0204 from the Deutsches Zentrum für Luft- und Raumfahrt e.V. (DLR).

References

Baldry, I. K., & Bedding, T. R. 2000, MNRAS, 318, 341
Balona, L. A., & Zima, W. 2002, MNRAS, 336, 873
Bangulo, S., Landi Del'Innocenti, E., Landolfi, M., & Leroy, J. L. 1995, A&A, 295, 459
Bigot, L., & Dziembowski, W. A. 2002, A&A, 391, 235
Butler, R. P., Marcy, G. W., Williams, E., et al. 1996, PASP, 108, 500
Cunha, M. S., & Gough, D. 2000, MNRAS, 319, 1020
Cunha, M. S. 2001, MNRAS, 325, 373
Dziembowski, W. A., & Goode, P. R. 1996, ApJ, 458, 338
Gabriel, M., Noels, A., Scuflaire, R., & Mathys, G. 1985, A&A, 143, 206
Gautschy, A., Saio, H., & Harzenmoser, H. 1998, MNRAS, 301, 31
Hatzes, A. P., & Kürster, M. 1994, A&A, 285, 454
Hatzes, A. P., Kanaan, A., & Mkrtichian, D. E. 1999, in Precise Stellar Radial Velocities, ed. J. B. Hearnshaw, & C. D. Scarfe (San Francisco: Sheridan Books), IAU Coll. 170, ASP Conf., 185, 166
Hatzes, A. P., Mkrtichian, D. E., & Kanaan, A. 2002, in Radial and Nonradial Pulsations as Probes of Stellar Physics, ed. C. Aerts, T. Bedding, & J. Christensen-Dalsgaard (San Francisco: Sheridan Books), IAU Coll. 185, ASP Conf. Ser., 259, 300
Hatzes, A. P., & Mkrtichian, D. E. 2005, A&A, 430, 279
Kanaan, A., & Hatzes, A. P. 1998, ApJ, 503, 848
Kochukhov, & Ryabchikova 2001a, A&A, 374, 615
Kochukhov, O., & Ryabchikova, T. 2001b, A&A, 377, L22
Kürster, M., Schmitt, J. H. M. M., Cutispoto, G., & Dennerl, K. 1997, A&A, 320, 831
Kurtz, D. W. 1978, IBVS, 1436
Kurtz, D. W. 1982, MNRAS, 200, 807
Kurtz, D. W., & Seeman, J. 1983, MNRAS, 205, 11
Kurtz, D. W., & Shibahashi, H. 1986, MNRAS, 223, 557
Kurtz, D. W., & Marang, F. 1987, MNRAS, 229, 285
Kurtz, D. W., Matthews, J. M., Martinez, P., et al. 1989, MNRAS, 240, 881
Kurtz, D. W., Kawaler, S. D., Riddle, R. L., et al. 2002, MNRAS, 330, L57
Kurtz, D. W., Elkin, W. G., & Mathys, G. 2003, MNRAS, 343, L5
Leroy, J. L., Landolfi, E., & Landi Del'Innocenti, E. M. 1996, A&A, 311, 513
Lomb, N. R. 1976, Ap&SS, 39, 477
Matthews, J. M., Wehlau, W. H., Walker, G. A. H., & Yang, S. 1988, ApJ, 324, 1099
Matthews, J. M., Kurtz, D. W., & Martinez, P. 1999, ApJ, 511, 422
Mkrtichian, D. E. 1992, in Magnetic Stars, ed. Yu. V. Glagolevsky, & I. I. Romanyuk (Sankt-Petersburg: Nauka), 260
Mkrtichian, D. E. 1994, Sol. Phys., 152, 275
Mkrtichian, D. E., Hatzes, A. P., & Panchuk, V. E. 2000, in Variable Stars as Essential Astrophysical Tools, ed. C. Ibanogly (Dordrecht: Kluwer), NATO Science Ser., Math. Phys. Sci., 544, 405
Mkrtichian, D. E., & Hatzes, A. P. 2000, in The Impact of Large-Scale Surveys on Pulsating Star Research, ed. L. Szabados, & D. Kurtz (San Francisco: Sheridan Books), IAU 176, ASP Conf. Ser., 203, 455
Mkrtichian, D. E., Hatzes, A. P., & Kanaan, A. 2003, MNRAS, 781
Murdoch, K. A., Hearnshaw, J. B., & Clark, M. 1993, ApJ, 413, 349
Preston, G. W. 1972, ApJ, 175, 465
Ryabchikova, T. A., Landstreet, J. D., Gelbman, M. J., et al. 1997, A&A, 327, 1137
Saio, H., & Gautschy, A. 2004, MNRAS, 350, 485
Savanov, I. S., Malanushenko, V. P., & Ryabchikova, T. A. 1999, Astron. Lett., 25, 902
Scargle, J. D. 1982, ApJ, 263, 835
Shibahashi, H. 1984, Mem. Soc. Astron. Ital., 55, 181
Takata, M., & Shibahashi, H. 1995, PASPJ, 47, 219
Tassoul, M. 1990, ApJ, 358, 313
Tull, R. G., MacQueen, P. J., Sneden, C., & Lambert, D. L. 1995, PASP, 107, 251
Valenti, J. A., Butler, R. P., & Marcy, G. W. 1995, PASP, 107, 966